J. Coat. Technol. Res.
https://doi.org/10.1007/s11998-024-00989-2

In situ grown gluconate-containing CaAl-LDH/organic coating for steel corrosion protection

Muhammad Ahsan Iqbal, Cristina Neves, Maksim Starykevich, Roberto Martins, Mário G. S. Ferreira, Joao Tedim

Received: 19 February 2024 / Revised: 20 June 2024 / Accepted: 23 June 2024

Abstract This study reports the development of anticorrosive bilayer coatings consisting of in situ grown layered double hydroxides (LDH) covered with a polyurethane layer on a steel substrate. This design aims at providing corrosion protection via the controlled release of gluconate from LDH near the substrate, while at the same time contributing to the improvement of the polyurethane layer coating adhesion. The CaAl-LDH thin film was initially grown directly on AISI 1080/1010 carbon steel and modified with environmentally friendly gluconate molecules through an ion-exchange reaction. The effect of polyurethane treatments on the LDHs thin film was systematically explored: gluconate is either intercalated in LDHs or dispersed in polyurethane coatings, and the two systems are studied to understand the role of inhibitors in bilayer coating systems at defined conditions. The structural characteristics of the developed coatings were evaluated by scanning electrochemical microscopy (SEM), X-ray diffraction (XRD), Fourier transform infrared spectroscopy (ATR-FTIR), and glow discharge optical microscopy (GDOES). The findings of electrochemical impedance spectroscopy (EIS) measurements on coated carbon steel substrates in NaCl solution demonstrated the significance of the bilayer film design for long-term corrosion protection, by combining active corrosion protection provided by the LDH conversion film with the passive barrier effect against electrolyte species rendered by the organic polyurethane layer. Additionally, improving the polyurethane coating's wet adhesion to the substrate when applied onto CaAl-LDH opens new directions toward the co-development of surface treatments with organic coatings.

Keywords CaAl-LDH, Gluconate corrosion inhibitor, Organic coating, Electrochemical impedance spectroscopy

Introduction

Steel is a structural material used worldwide in various industrial fields, from building constructions to offshore platforms and the vehicle industry. However, when exposed to an aggressive environment, steel becomes susceptible to corrosion.[1–4]

A wide range of strategies can be employed to protect metals against corrosion, from corrosion inhibitors to cathodic and/or anodic protection, and the application of organic protective coatings. The latter is one of the most general and cost-effective measures to avoid the degradation of active metals by corrosion.[5–9] However, even when organic coatings are used, water, ions, and oxygen can penetrate the organic coating through pores, cracks, and other defects that may form during exposure, enabling conductive pathways of electrolyte species toward the metal/coating interface and leading to corrosion onset.[10,11]

As a result, there is a need to impart active corrosion protection functionality to the organic coating by

Supplementary Information The online version contains supplementary material available at https://doi.org/10.1007/s11998-024-00989-2.

M. A. Iqbal (✉), C. Neves, M. Starykevich, M. G. S. Ferreira, J. Tedim (✉)
Department of Materials and Ceramic Engineering, CICECO-Aveiro Institute of Materials, University of Aveiro, 3810-193 Aveiro, Portugal
e-mail: muhammadahsan.iqbal@ua.pt

J. Tedim
e-mail: joao.tedim@ua.pt

R. Martins
CESAM-Centre for Environmental and Marine Studies, Department of Biology, University of Aveiro, 3810-193 Aveiro, Portugal

Published online: 20 September 2024

incorporating corrosion inhibitors. This can be simply achieved by directly adding corrosion inhibitors in the organic coating systems.[12–15] Nonetheless, the direct addition of corrosion inhibitors encloses various disadvantages: it may lead to the spontaneous leaching of species, limiting the long-term protection, and corrosion inhibitors may detrimentally interact with the coating matrix, decreasing its overall performance.[16] On the other hand, the development and incorporation of micro/nanocontainers carrying inhibitors into the organic coating matrix have become a widely accepted alternative to the direct addition of inhibitors, as these reservoirs are designed to store and release the corrosion inhibitors in a controlled manner.[17–21]

One class of materials studied considerably as nanocontainers for corrosion protection in the last two decades is the layered double hydroxide (LDH).[22–26] LDH-based nanocontainers are regarded as one of the most promising systems for the development of smart coating systems due to their distinct lamellar structure, ion-exchange behavior, memory effect, and self-healing properties. Indeed, LDH can be produced as colloidal particles in different physical states (e.g., as powder or paste) and directly added as a functional nanoadditive pigment to organic coatings. Alternatively, they may be grown in situ on the metal substrate as a conversion layer via electrochemical or hydrothermal treatments[27,28] or deposited as an inorganic film using different techniques such as electrophoretic deposition or spin coating.[29] So far, most research of in situ grown LDH films is mainly focused on light metal alloys, mainly because the type of metal cations provided by these substrates give rise to stable well-known LDH conversion films (e.g., Mg-Al, Zn-Al LDH). Tabish et al. reported the development of CaAl-LDH intercalated with 2-mercaptobenzothiazole (MBT) and incorporated them at different concentrations in organic coatings as a pigment to enhance the corrosion protection of steel.[30] Holzner et al.[31] investigated the mechanism and kinetics of MgAl-LDH conversion layer formation on ZM-coated steel and reported the influence of the LDH conversion layer on the corrosion resistance of ZM-coated steel. Dong et al. investigated the growth mechanism of Co-Al-LDH film grown in situ on a steel substrate and demonstrated an increase in the corrosion resistance of steel.[32] Hydrocalumite minerals have corrugated brucite-like layers with Ca^{2+} and Al^{3+} ions arranged seven- and six-coordinated in a 2:1 ratio, respectively. In this study, Ca^{2+} and Al^{3+} were used as divalent and trivalent cations to synthesize Ca-Al-LDH on a steel substrate. Conversely, the investigation of LDH developed in situ on carbon steel and its relationship with organic coating systems is a topic worth discussing, particularly the role of inhibitors in the bilayer system. It is uncertain how corrosion inhibitors, whether directly incorporated in the organic coating or intercalated in the LDHs, contribute to enhancing the ability of a bilayer coating approach for the protection of carbon steel. Furthermore, the wet adhesion properties of organic coatings, when in contact with corrosive solutions are unreliable, which can impact long-term corrosion resistance. The role of in situ developed LDH films on carbon steel, as well as their interaction with organic coating systems, must be investigated in order to address issues of wet adhesion loss and overall system stability, where the organic coating when in contact with a high surface roughness LDH thin film, soaks into its nanosheet and provides better adhesion properties to the substrate.

Therefore, this work describes the development of CaAl-LDH thin film modified subsequently with gluconate anions. In addition, we investigate how the Ca-Al LDH film interacts with a polyurethane coating layer and how this bilayer system renders corrosion protection to the carbon steel substrate. Specifically, the anticorrosion effect of this bilayer coating system and the subsequent impact of gluconate, either dispersed in polyurethane coating or intercalated in LDH film, is investigated and described. Various corrosion inhibitors have been widely employed to study their protective properties and unveil the inhibition mechanisms against steel corrosion.[33–36] The present study is focused on the utilization of gluconate. This non-toxic biomolecule is reported as an efficient inhibitor against the corrosion of tin, iron, and mild steel in near pH-neutral media.[37,38] The choice of the inhibitor was motivated by stringent environmental and ecological rules to replace traditional toxic compounds found to be hazardous to society.[39,40] This paper describes the preparation and modification of CaAl-LDH film directly on carbon steel, as well as inhibitor performance in different layers of a bilayer system using polyurethane coating as a model system while taking into account the overall system's dry and wet adhesion characteristics.

Materials and methods

Materials

AISI1008/1010 carbon steel plates with dimensions (4 cm × 1 cm × 0.5 cm) were used as substrate material for the growth of Ca-Al LDH. Initially, the steel samples were mechanically ground with up to 2000# grits of SiC abrasive paper, degreased with acetone, rinsed with ethanol, and dried with compressed air. The following analytical grade was used as reagents for the synthesis of the CaAl-LDH film: $CaNO_3{\cdot}4H_2O$, $Al(NO_3)_3{\cdot}9H_2O$, NH_4NO_3, and NaOH (supplied by Sigma-Aldrich Corporation, purity ≥ 98%). A commercial two-component polyurethane (lacquer AQ CC

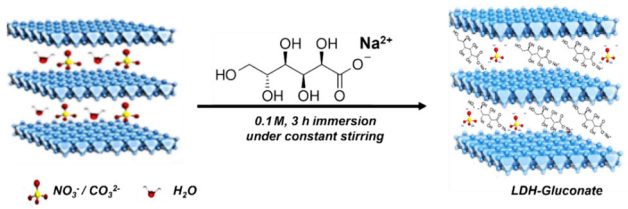

Fig. 1: Schematic representation of LDHs as-prepared structure

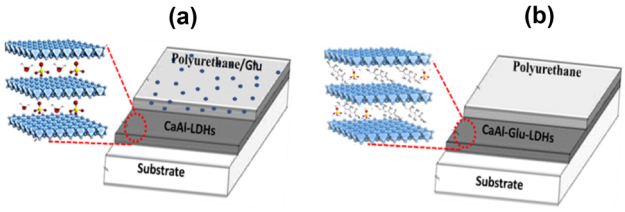

Fig. 2: Schematic diagram of the developed composite coatings. (a) LDH/Polyurethane-Glu, (b) LDH-Glu/ Polyurethane

150 and hardener AQ BU 13, supplied by Synpo a.c.) was used to develop the organic coating layer.

Preparation of coatings

Preparation of Ca-Al-LDH-films

The CaAl-LDH were synthesized by an in situ growth method by preparing the mixed solution composed of 0.1 M $Ca(NO_3)_2{\cdot}4H_2O$, 0.05 M of $Al(NO_3)_3{\cdot}9H_2O$, and 0.3 NH_4NO_3, purged with nitrogen gas for 15 min and were transferred in a Teflon-lined stainless steel autoclave containing the pretreated steel samples. The pH of the solution was adjusted to 12.0 before the autoclave was closed and heated for 18 h at 140°C. Finally, the CaAl-LDH coated samples were washed with distilled water and dried at ambient temperature. To prepare CaAl-Gluconate-LDH, the steel plates with Ca-Al-NO_3 LDH specimens were dipped in a 0.1 M solution of sodium gluconate (abbreviated hereafter as Glu) for 3 h under stirring. Then, the specimens were washed with distilled water and were dried in the oven at 60°C for 30 min. Figure 1 presents a schematic illustration of LDH structural formation and modification with gluconate via ion-exchange process.

Preparation of bilayer coating

The commercial lacquer AQ CC 150 was added to the curing agent (AQ BU 13) with a mass ratio of 2.5:1 and mixed uniformly through mechanical stirring. The polyurethane coatings were applied on the CaAl-Gluconate-LDHs film with the help of a bar coater (50 μm nominal thickness). The resulting coatings are named *LDHs-Glu/Polyurethane*. In parallel, *LDHs/ Polyurethane-Glu* coatings were also prepared by applying a similar polyurethane coating with dispersed gluconate inhibitors (3 wt%) on the CaAl-LDHs film. The concentration of gluconate was adjusted after the initial screening of different gluconate dispersions in polyurethane coatings based on impedance and porosity characteristics. The curing in both cases was done for 10 min at 25°C and then for 40 min at 80°C using an oven. Figure 2 represents the general design of developed LDHs/Polyurethane-based coating systems. For reference, the pure polyurethane coating was prepared directly on the steel surface without any inhibitors. Table 1 describes the general terms used hereafter for the developed specimens.

Characterization

The morphology and microstructural features of the obtained LDH films were analyzed by scanning electron microscopy (JEOL IT300) operated at 10 kV accelerating voltage. The XRD characterization of the developed samples was performed using a PANalytical X'Pert diffractometer (CuKα1 radiation, λ = 0.154056 nm; a tube power of 45 kV and 40 mA) coupled with a PIXcell1D detector, following a step of 0.02° over an angular range between 3.5° and 90°. FTIR was conducted in attenuated total reflectance (ATR) mode with an Excalibur series instrument to analyze the surface functional groups and the chemical bonding of the samples within the wavenumber range from 550 to 4000 cm^{-1} with a 4 cm^{-1} resolution and 32 scans; a diamond crystal was used as the internal reflective element and complement the structural analysis by XRD.

To investigate the elemental depth profile of LDH films, glow discharge optical emission microscopy (GDOES) was performed at an accelerating voltage of 200 kV.

Electrochemical studies of the coated substrates were carried out by electrochemical impedance spectroscopy (EIS). EIS was conducted with Gamry FAS2 Femtostat (Gamry Instruments, USA) coupled to a PCI4 controller at open circuit potential (OCP) with the application of a 10-mV sinusoidal perturbation in the 10 kHz to 10 mHz frequency range, taking 7 points per decade. A configuration of three-electrode systems, i.e., saturated calomel electrode (SCE)/reference electrode, platinum/counter electrode, and coated steel sample/working electrode in 0.05 M NaCl solution, was used to measure the EIS analysis.

Adhesion tests (ASTM D 3359-09e2/ DIN EN ISO 2409) were carried out through the cutting tool (crosshatch cutter test kit) fitted with a blade tooth spaced at 1.0 mm apart and were used to make a cross-

Table 1: Developed coating specimens on AISI 1008/1010 carbon steel substrates

Designation	Description
LDH	CaAl-LDH grown on the steel surface
LDH-Glu	CaAl-Gluconate-LDH grown on the steel surface
LDH/Polyurethane-Glu	Top layer of Gluconate dispersed polyurethane coating applied onto CaAl-LDH
LDH-Glu/Polyurethane	Top layer of pure polyurethane coating applied onto CaAl-Gluconate-LDH
Reference	Pure polyurethane coating applied directly on the carbon steel surface

cut pattern through the composite coatings at ca. 90° angles. Pressure-sensitive tape was then applied and removed to assess the coating quality by observing the coating behavior to the tape removal.

Results and discussion

Figure 3 shows the XRD patterns of substrates after the growth of LDH and LDH-Glu. The pattern indicates a series of 2θ peaks related to the LDH phase with the possible characteristic reflections of the CaAl-LDH. These reflections support the successful preparation of the CaAl-LDH hydrocalumite-like structure.[41,42] The presence of a peak at 11.67° with the *d*-spacing value of 0.76 nm, calculated from Bragg's Law, may be due to the intercalation of CO_3^{2-} in the LDH galleries.[41,43,44] This finding is not unexpected: the solution on which LDH was grown had an initial pH of 12 and, although having used a flow of nitrogen gas to reduce the amount of CO_2 dissolved in water, its complete removal may not have occurred.

After modification with gluconate, the at-low 2θ reflections shifted toward lower angles, indicating the intercalation of gluconate anions inside the LDH interlayers. The basal plane spacing of LDH-Glu, estimated from the positions of the fundamental characteristic peak (00l), is 0.95 nm. It is also worth noting that the basal spacing associated with developed LDH-Glu film in the present work is lower than that synthesized by the coprecipitation method.[37] This may be due to the difficulty in achieving a complete exchange with carbonates, which agrees with previous studies.[25,45]

The GDOES depth profiles for the developed specimens are shown in Figure 4. The depth profile can be divided into three main regions: *zone 1*—LDH layer; *zone 2*—transition from the LDH layer to the substrate; and zone *3*—substrate. For CaAl-LDH, O, N, Ca, and Al signals are intense in zone 1, indicating their enrichment on the surface, and are consistent with the XRD description. It is worth noting that the signal from N is much more intense than the signal from C, which may imply that nitrates are still present in the film, either adsorbed in the outer surface of LDH or some amorphous regions of the layer, while the presence of NO_3^- also cannot be fully excluded.

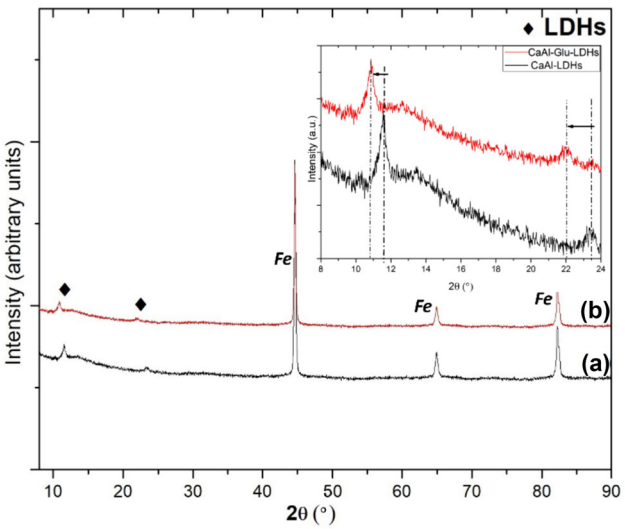

Fig. 3: XRD patterns of LDH films (a) LDH, (b) LDH-Glu

Furthermore, in *zone 2*, there is a decrease of Ca and Al signals and an increase of Fe, showing that this is a transition between the LDH film and an iron-oxide/hydroxide region. In *zone 3*, all the signals decrease except for Fe, indicating that the carbon steel substrate has been reached.

After the exposure of the LDH film to the gluconate solution, the signal of C is more prominent in the sample. In *zone 1*, signals of Ca, Al, O, N, H, and C (to some extent) are the most intense. The increase of C, H and O may be associated with the presence of gluconate. In *zone 2*, all these signals decrease while the signal from Fe increases, and in *zone 3*, the most intense signal comes from Fe. The reduced sputtering time to reach *zone 3* after ion exchange with gluconate (LDH-Glu) described the LDH dissolution during immersion in gluconate base solution and was characterized by the thinning of LDH film after ion exchange.

The FTIR spectra of the pristine LDH samples are shown in Fig. 5. A broad, intense band observed in the 3000–3800 cm^{-1} range is due to the OH stretching mode, and the band is broadened because of the superposition of various hydrogen bonds with interlayer water molecules and interlayer anions.[46] The band at 1630 cm^{-1} is attributed to the deformation mode of the interlayer water molecules. The band in

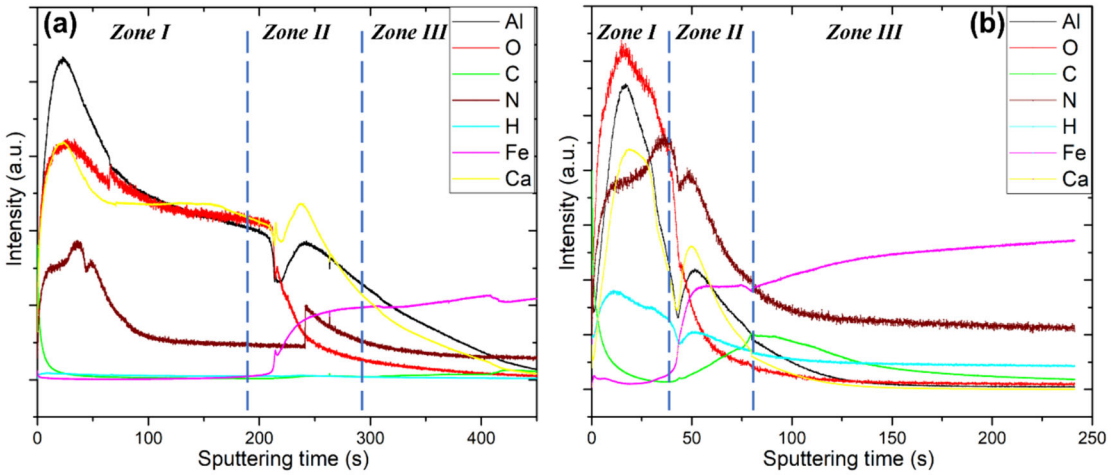

Fig. 4: GDOES depth profile of samples: (a) LDH, (b) LDH-Glu

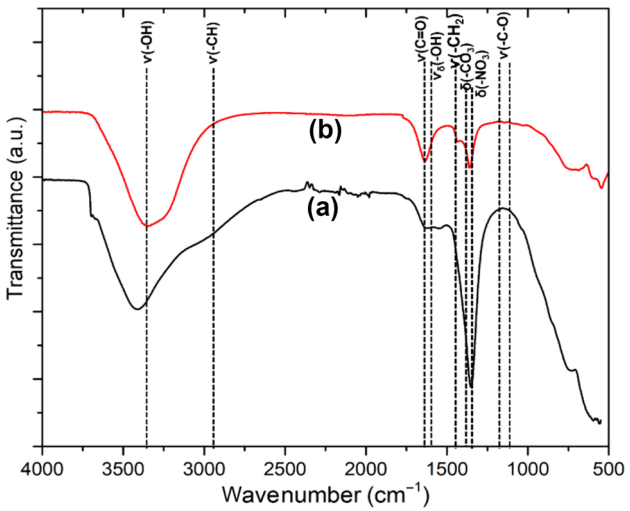

Fig. 5: FTIR spectra: (a) LDH, (b) LDH-Glu

the 1350 cm^{-1} region can be attributed to the vibration modes of CO_3^{2-} or NO_3^- or the overlap of both bands in the region ranging from 1350 to 1400 cm^{-1}.[47] The 1576 cm^{-1} band originates from the H_2O bending in the interlayer, and the carbonate anion adsorption band at 1440 cm^{-1} overlapped with the 1347 cm^{-1} band related to the nitrate group stretching.[48] The vibration mode near 440 cm^{-1} was assigned to the vibration mode of metal-oxygen in layered double hydroxide. Compared to the sample LDH (i.e., before ion exchange), the LDH-Glu spectrum shows the asymmetric stretching vibration mode of C=O at 1634 cm^{-1}, along with the presence of a peak at 1427 cm^{-1} and out-of-plane bending vibration mode, c(OH), at 660 cm^{-1} suggesting the existence of species containing carboxylic groups.[49] In comparison, the additional (–CH) peak indicates the presence of gluconate inside LHDs. These results show that the gluconate anions are present in LDH films, with no critical modifications to the LDH structure upon ion exchange.

Figure 6 shows SEM images of obtained LDH films before (panel a) and after (panel b) modification with gluconate. The LDH films reveal plate-like morphology perpendicular to the substrate, like other LDH films grown in different substrates.[49] The films obtained do not show surface defects, such as large pores or uncovered surface regions, and the morphology does not suffer key changes upon treatment with the gluconate solution.

In addition, the top view SEM images of the bilayer coating systems after application of the polyurethane coating layer are presented in panels (c) and (d). In the case of the LDH-Glu/Polyurethane system (panel c), the polyurethane seems to cover the LDH film, while in the system LDH/Polyurethane-Glu, there are several defects with open pores (panel d). The latter observation can be due to the poor interaction between sodium gluconate salt and the polyurethane layer.

EIS was employed to evaluate the corrosion performance of these bilayer systems, exposing coated carbon steel samples to a 0.05 M NaCl aqueous solution for different immersion times. The Bode representation of the EIS spectra acquired is presented in Fig. 7. Panels a and b show the EIS spectra for all the systems studied after 1 h of immersion. The system with the lowest impedance magnitude corresponds to the uncoated steel. It is possible to detect two overlapped time constants at intermediate frequencies between 10^0 and 10^2 Hz, which may be ascribed to ongoing corrosion processes and mass-transport controlled processes.[50] When the LDH is grown, the substrate becomes more protected: the impedance magnitude increases across the whole frequency domain, with an additional time constant detected at high frequencies that can be ascribed to the LDH layer (around 10^4 Hz), followed by a second time constant associated with ongoing corrosion processes (around 10 Hz). When the LDH layer is modified with gluconate (LDH-Glu), the low and intermediate fre-

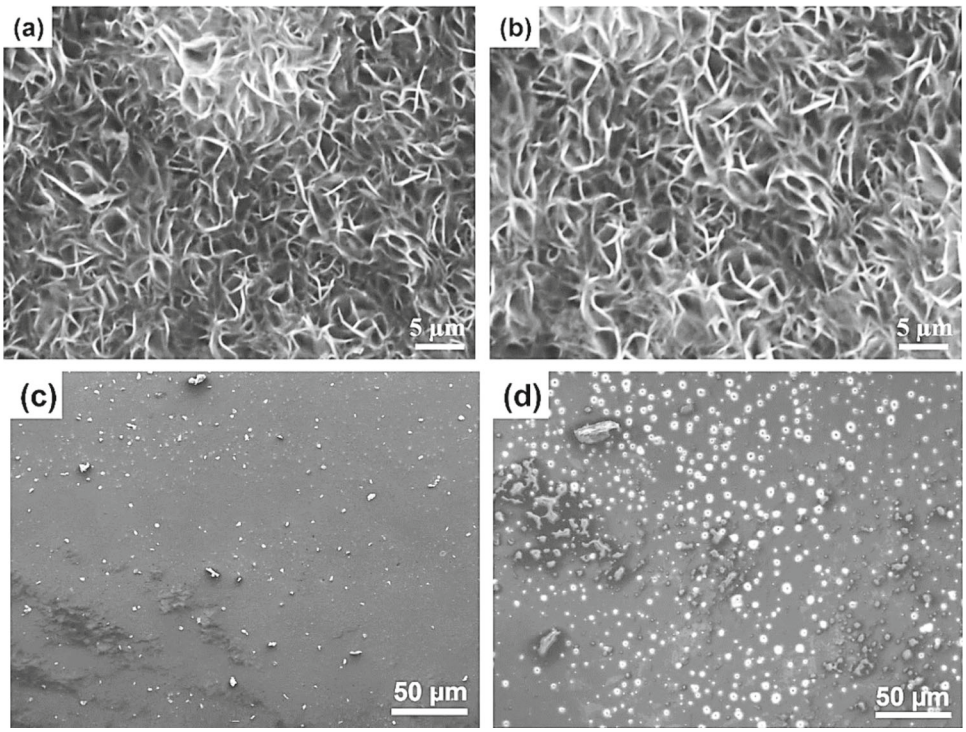

Fig. 6: SEM images: (a) LDH, (b) LDH-Glu, (c) LDH-Glu/Polyurethane, (d) LDH/Polyurethane-Glu

quency impedance magnitude increases, which may anticipate the role of gluconate as a corrosion inhibitor of steel. On the other hand, the high-frequency time constant initially detected for LDH seems to occur now at lower frequencies (around 10^2 Hz). This may imply that a thinning of the LDH layer could have occurred during the exposure of the LDH layer to the gluconate-containing solution (consistent with previous description of GDOES results) or that, at least from an electrochemical standpoint, the region of the LDH layer that offers resistance against ingress of electrolyte may be thinner. Only one-time constant is detected when the LDH layer is covered with polyurethane coating, which can be assigned to the organic coating response.[51] The positive effect of combining the LDH layer with the polyurethane layer (LDH-Glu/Polyurethane and LDH/Polyurethane-Glu) vs. polyurethane layer directly applied onto the carbon steel substrate (Polyurethane) is also clear: the impedance magnitude of the polyurethane system alone is several orders of magnitude lower than the LDH-polyurethane system across the whole range of frequency. In addition to the potential barrier effect of the LDH thin film, there may also be an important role in the adhesion of the organic layer to the substrate covered with the LDH film.

The long-term protective effect of the bilayer system was also surveyed. The Bode plots of EIS spectra obtained for LDH/Polyurethane-Glu and LDH-Glu/Polyurethane after 24, 72, 168, 240, and 480 h are depicted in Fig. 7 (panels c to f). LDH-Glu/Polyurethane system displayed higher impedance magnitude after 1 h of immersion when compared to the LDH/Polyurethane-Glu system. This trend was also observed for longer times of immersion. Nonetheless, when looking at the decrease in impedance magnitude for different immersion times, especially at low frequencies, this decrease was more significant for the coating where gluconate had been directly added to the polyurethane layer when compared to the system where gluconate was present in the LDH film. The interpretation of these changes may be rooted in differences in coating permeability to electrolyte species. Indeed, recalling Fig. 6, pores were detected in the system where gluconate had been directly added to the polyurethane layer. This opened structure facilitates the ingress of electrolyte species and may contribute to lowering pore resistance (to be discussed later). Furthermore, the direct addition of a water-soluble salt to the polyurethane-coated specimen can create further osmotic pressure, forcing a higher water ingress than in the polyurethane layer without sodium gluconate.[52]

Figure 8 summarizes the variation of impedance magnitude at low frequencies (0.01 Hz) from 1 to 480 h of immersion, and whether it is assumed that this value is related to the corrosion rate, the positive effect of combining LDH with Polyurethane is demonstrated. However, the LDH-Glu/Polyurethane system is the most protective under the conditions tested.

The EIS spectra presented in panels ''c'' to ''f'' of Fig. 7 were fitted using Echem Analyst software, and the results are shown in Tables 2 and 3, using two different equivalent circuit models presented in Fig. 9. The electrical circuits that were used in the fitting of

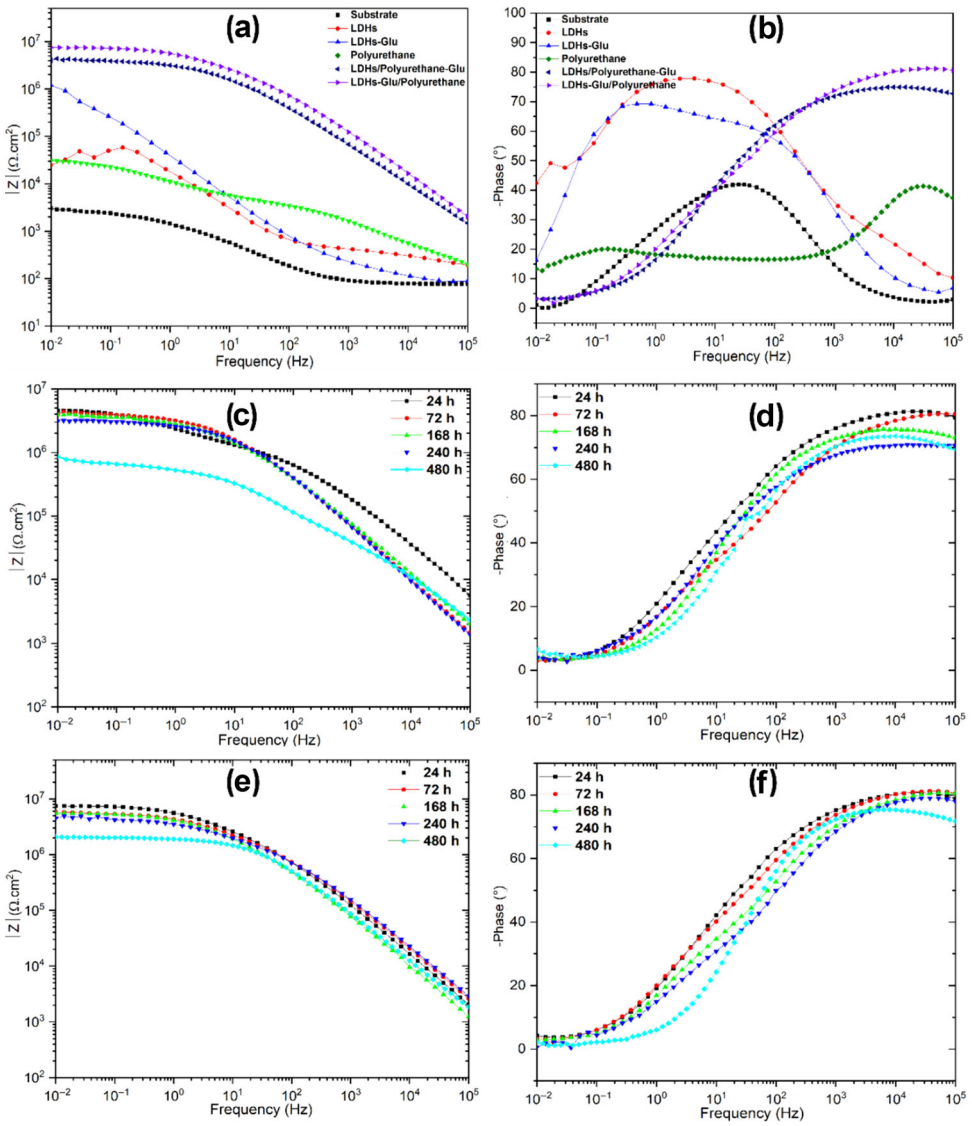

Fig. 7: EIS spectra of developed coating systems: (a, b) coatings after 1 h immersion, (c, d) LDH/Polyurethane-Glu, (e, f) LDH-Glu/Polyurethane

EIS experimental data from the bilayer coatings were studied to measure important impedance characteristics. Solution resistance, pore resistance 1 and pore resistance 2 are related to the inner and external parts of the film and are represented by R_s, R_{coat1}, and R_{coat2} in the suggested equivalent circuits. The related constant phase elements are represented by CPE_{coat1} and CPE_{coat2} respectively, and α is the exponent of CPE. In the case of LDH/Polyurethane-Glu, only a one-time constant is detected, except for 24 h immersion. The high-frequency time constant can be associated with the organic coating, while the additional time constant detected for 24 h of immersion may be ascribed to the inner coating layer (LDH), which is no longer noticed as a separate layer for longer immersion times. This second-time constant occurs around 10^1–10^2 Hz and is not well seen due to partially overlapping with the high-frequency one. However, two-time constants provide reliable fitting in this region of the frequency domain. Although the equivalent circuits used for the two coating systems were not always the same, Tables 2 and 3 demonstrate that the total coating pore resistance, or R coat, as determined by Rcoat1 + Rcoat2, is consistently greater for LDH-Glu/Polyurethane than LDH-Polyurethane/Glu. It is difficult to assign time constants from a physicochemical perspective. The effective capacitance was calculated using equation (1) derived by Hsu and Mansfeld,[53] and the corresponding values are depicted in Tables 2 and 3.

$$C_{\text{eff}} = Q^{(1/a)} R^{(1-a)/a} \tag{1}$$

where α and Q are frequency-independent parameters of the CPE and R the parallel resistance-associated.

In the case of LDH-Glu/Polyurethane and for LDH/Polyurethane-Glu after 24 h, the order of magnitude associated with C_{eff} for both the first and second-time constants is consistent with a coating layer response. A possible rationalization for this behavior may be that the external layer is composed of polyurethane only, whereas the inner coating layer response results from a combination of organic polyurethane/inorganic LDH-Glu that remains stable throughout the immersion period monitored.

The appearance of the developed specimens on carbon steel plates before and after immersion for 480 h is shown in the supplementary section. The corrosion products are visible on the substrates of LDH and LDH-Glu developed plates, where corrosive species covered the whole substrate after 20 days of contact with the electrolyte. The LDH/Polyurethane coatings have shown localized corrosion and corrosion products on the surface, however, the coatings appeared to be stable and intact with the substrate, and no specific swelling is observed in the coating systems. At the same time, red rust spots were observed in some areas, specifically in the case of LDH/Polyurethane-Glu. It is worth noting that the equivalent circuits presented earlier do not account for an additional time constant associated with corrosion processes that led to the formation of corrosion spots underneath the organic coatings and are visually

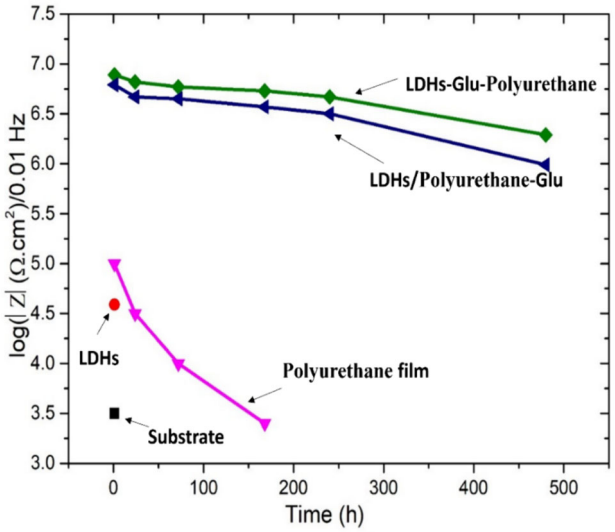

Fig. 8: Impedance modulus of studied surfaces at 0.01 Hz against various immersion times

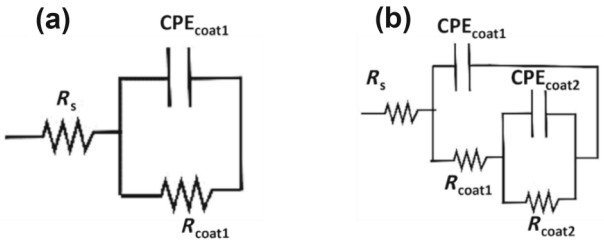

Fig. 9: Equivalent circuit used to fit the EIS results

Table 2: EIS fitting results for LDH/Polyurethane-Glu

Immersion time (min)	CPEcoat$_1$ Ω^{-1} cm^{-2} s$^{\alpha}$	R_{coat1} Ω cm^2	α_{coat}	Ceff Fcm^{-2}	CPE$_{coat2}$ Ω^{-1} cm^{-2} s$^{\alpha}$	R_{coat2} Ω cm^2	α_{coat2}	Ceff Fcm^{-2}	R_{coat} Ω cm^2
24	4.87×10^{-9}	5.66×10^{5}	0.78	9.60×10^{-10}	1.71×10^{-7}	5.50×10^{6}	0.40	1.56×10^{-7}	6.06×10^{6}
72	1.58×10^{-8}	3.69×10^{6}	0.79	7.46×10^{-9}					3.69×10^{6}
168	2.13×10^{-8}	3.41×10^{6}	0.74	8.72×10^{-9}					3.41×10^{6}
240	1.36×10^{-8}	2.86×10^{6}	0.80	6.32×10^{-9}					2.86×10^{6}
480	3.59×10^{-8}	5.24×10^{5}	0.77	1.10×10^{-8}					5.24×10^{5}

Table 3: EIS fitting results for LDH-Glu/Polyurethane

Immersion time (min)	CPE$_{coat1}$ Ω^{-1} cm^{-2} s$^{\alpha}$	R_{coat1} Ω cm^2	α_{coat}	Ceff Fcm^{-2}	CPE$_{coat2}$ Ω^{-1} cm^{-2} s$^{\alpha}$	R_{coat2} Ω cm^2	α_{coat2}	Ceff Fcm^{-2}	R_{coat} Ω cm^2
24	2.78×10^{-9}	7.41×10^{5}	0.9	1.44×10^{-9}	2.80×10^{-8}	7.14×10^{6}	0.55	7.54×10^{-9}	7.8×10^{6}
72	2.44×10^{-9}	5.55×10^{5}	0.89	1.13×10^{-9}	3.70×10^{-8}	5.40×10^{6}	0.52	8.47×10^{-9}	5.9×10^{6}
168	4.27×10^{-9}	4.16×10^{5}	0.90	2.25×10^{-9}	3.67×10^{-8}	5.39×10^{6}	0.51	8.17×10^{-9}	5.8×10^{6}
240	2.49×10^{-9}	5.63×10^{5}	0.88	1.07×10^{-9}	4.86×10^{-8}	4.24×10^{6}	0.50	1.01×10^{-8}	4.8×10^{6}
480	8.85×10^{-9}	1.95×10^{6}	0.82	3.70×10^{-9}					1.9×10^{6}

detected after 480 h of immersion. This can be attributed to the fact that the barrier properties provided by the organic coating prevent the identification of these activities since the coating impedance remains high. Similar phenomenon has been observed in the literature and is attributed to the nature of the polymer that permits mostly water to permeate while the flow of ions across the coating is not yet considerable.[52]

The photographs of the specimens after adhesion tests are displayed in Fig. 10. The rating system (from 0 to 5) is based on the detached surface area after the test, considering 5 optimal (no detachment) and 0 complete detachments (> 65%). Before being submerged in a NaCl solution, the polyurethane coating alone exhibited high adherence; however, after ten days of immersion, the film showed poor adhesion, (rating ''1''). When exposed to corrosive electrolytes, corrosive ions penetrate and impair the polyurethane coating's barrier effectiveness, accelerating corrosion at the coating/substrate interface and causing increased delamination. The square grid pattern on the surface of the developed polyurethane coatings on the LDH surface indicates a rating of ''5'' for dry adhesion strength. This is because the polyurethane coating seeped into the nanosheet of the LDH thin film and

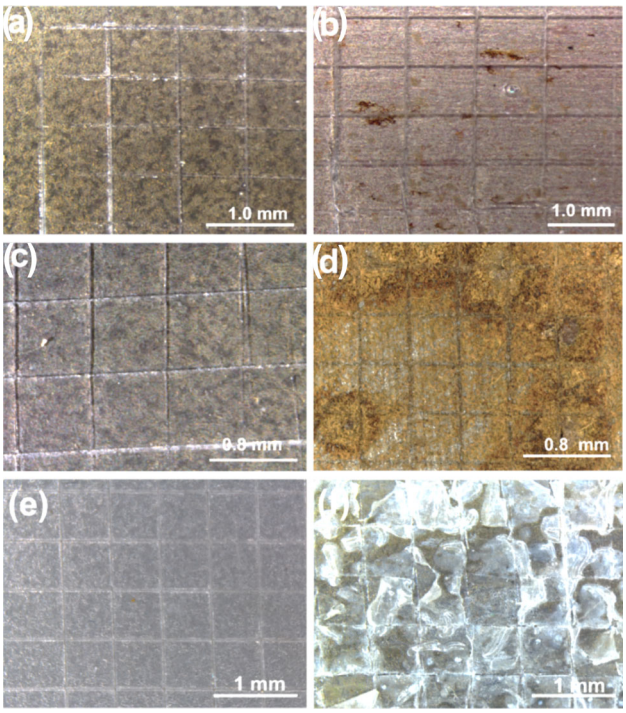

Fig. 10: Surface appearance of adhesion test for as-prepared coatings surfaces (a, c, e) and after 10 days of immersion in 0.05 M NaCl solution (b, d, f). (a, b) LDH-Glu/Polyurethane; (c, d) LDH/Polyurethane-Glu; (e, f) Polyurethane coating (reference)

may have bonded via strong interactions during the curing process, thereby improving the adhesion strength between the polyurethane coating and carbon steel substrate. After 10 days of immersion in 0.05 M NaCl solution, the LDH/Polyurethane-Glu showed some signs of adhesion loss and was considered as rating ''3'', however significantly better compared to the pure polyurethane coating applied directly onto carbon steel. The results showed that the LDH-Glu/Polyurethane had a significant role in improving the adhesion strength of the polyurethane layer. This is because the LDH film was used as a pretreatment for the polyurethane coating, and interfacial bonds between the LDH thin film and pure polyurethane coating play a significant role in improving the overall adhesion of the system. The corrosion product accumulation can be observed on LDH/Polyurethane-Glu for wet adhesion analysis, which is why LDH-Glu/Polyurethane coating performed better than LDH/Polyurethane-Glu. These changes in coating adhesion loss are then also reflected in the coating impedance analysis.

Based on the present findings, the polyurethane coatings provide initial strong barrier properties for both LDH-Glu/Polyurethane and LDH/Polyurethane-Glu, evidenced by the coating corrosion resistance properties investigated by EIS and visual inspection. Further, the presence of LDH limits interaction between corrosive species and the metallic substrate and delays the corrosion ions from reaching the metal substrate. Secondly, gluconate ions inside the system can be released to inhibit corrosion at the metal interface. Furthermore, it has been found that the direct incorporation of inhibitors into polyurethane coatings might induce degradation due to the adverse interaction between the polymer matrix and active species, and they have comparably weaker corrosion resistance properties than the LDH-Glu/Polyurethane system. The reason for the increase in corrosion resistance of the LDH-Glu/Polyurethane coating on carbon steel substrate can be due to the combined active and passive protection, arising from anion exchange between the inhibitor (gluconate) anions contained in the LDH and the aggressive Cl^- ions, and the organic coating barrier effect, respectively. The use of polyurethane coating directly on steel substrate reported a rapid decline of impedance values and adhesion failure. This demonstrates the notion of using LDH as a first layer to increase corrosion resistance and adhesion of the coating system. This is particularly noticeable when the initial layer of LDH contains inhibitor species, such as gluconate, in this example. The difference in impedance values between LDH-Glu/Polyurethane and LDH/Polyurethane-Glu points in the same direction as SEM and adhesion testing: gluconate does not work well when directly dispersed

in the polymer, but its effect when incorporated into the LDH film is more positive.

Conclusions

This study described the development of CaAl-LDH film grown directly on the surface of carbon steel, followed by the loading of gluconate. The surface morphologies of the CaAl-LDH revealed a uniform network of LDH lamellae, which provide a robust platform for modification with polyurethane coating. Two different strategies were followed to develop multifunctional coatings based on the addition of corrosion inhibitors, namely (a) LDH-Glu/Polyurethane, and (b) LDH/Polyurethane-Glu. The developed systems of LDH-Glu/Polyurethane and LDH/Polyurethane-Glu showed a positive effect in terms of steel protection against corrosion. Further, the presence of LDH film significantly improves the adhesion of the polyurethane coating to the metal substrate. The best system was found to be LDH-Glu/Polyurethane. The polyurethane layer renders a barrier effect against the initial transport of corrosion-relevant species (passive protection), while the LDH layer simultaneously provides corrosion inhibitor species (Glu) and entrapment of aggressive chloride ions (active protection). Above all, the presence of inhibitors in the protective LDH layer is a promising way to enhance the corrosion protection ability of bilayer coating systems where inhibitors are released closer to the substrate interface provide better corrosion protection compared to inhibitors directly added to the polyurethane coatings that can detrimentally lead to fast degradation of the polymeric layer. In real coating systems, the polymer layer will have to be loaded with additional anticorrosion pigments to render a long-lasting protection effect. Therefore, we propose that a combination of LDH-gluconate pretreatments with primers loaded with compatible anticorrosion pigments may be considered an environmentally friendly efficient coating design to protect carbon steel.

Funding The present work was carried out in the framework of the NANOGREEN project (CIRCNA/BRB/0291/2019) funded by national funds (OE) through FCT (Fundação para a Ciência e a Tecnologia, I.P.), as well as the COAT4LIFE project funded by the European Union's Horizon 2020 research and innovation programme under the Marie Skłodowska-Curie grant agreement No 101007430. Roberto Martins is funded by national funds (OE), through FCT (grant 2021.00386.CEECIND). We also acknowledge the financial support to CICECO (UIDB/50011/2020, UIDP/50011/2020 & LA/P/0006/2020) and to CESAM (UIDP/50017/2020 + UIDB/50017/2020 + LA/P/0094/2020) and by FCT/MCTES through national funds.

Conflict of interest The authors declare no conflict of interest.

References

1. Wang, Y, Wang, W, Liu, Y, Zhong, L, Wang, J, ''Study of Localized Corrosion of 304 Stainless Steel Under Chloride Solution Droplets Using the Wire Beam Electrode.'' *Corros. Sci.*, **53** (9) 2963–2968 (2011)
2. Döner, A, Solmaz, R, Özcan, M, Kardaş, G, ''Experimental and Theoretical Studies of Thiazoles as Corrosion Inhibitors for Mild Steel in Sulphuric Acid Solution.'' *Corros. Sci.*, **53** (9) 2902–2913 (2011)
3. Wang, Y, Wharton, JA, Ajit Shenoi, R, ''Ultimate Strength Analysis of Aged Steel-Plated Structures Exposed to Marine Corrosion Damage: A Review.'' *Corros. Sci.*, **86** 42–60 (2014)
4. Kurth, JC, Krauss, PD, Foster, SW, ''Corrosion Management of Maritime Infrastructure.'' *Transp. Res. Rec.*, **2673** (12) 2–14 (2019)
5. Kamimura, T, Hara, S, Miyuki, H, Yamashita, M, Uchida, H, ''Composition and Protective Ability of Rust Layer Formed on Weathering Steel Exposed to Various Environments.'' *Corros. Sci.*, **48** 2799–2812 (2006)
6. Bouanis, M, Tourabi, M, Nyassi, A, Zarrouk, A, Jama, C, Bentiss, F, ''Corrosion Inhibition Performance of HCl Solution: Gravimetric, Electrochemical and XPS Studies.'' *Appl. Surf. Sci.*, **389** 952–966 (2016)
7. Zhou, Y, Zuo, Y, Lin, B, ''The Compounded Inhibition of Sodium Molybdate and Benzotriazole on Pitting Corrosion of Q235 Steel in NaCl+$NaHCO_3$ Solution.'' *Mater. Chem. Phys.*, **192** 86–93 (2017)
8. Yabuki, A, Shiraiwa, Fathona, IW, ''pH-Controlled Self-Healing Polymer Coatings with Cellulose Nanofibers Providing an Effective Release of Corrosion Inhibitor.'' *Corros. Sci.*, **103** 117–123 (2016)
9. Zhang, D, Qian, H, Wang, L, Li, X, ''Comparison of Barrier Properties for a Superhydrophobic Epoxy Coating Under Different Simulated Corrosion Environments.'' *Corros. Sci.*, **103** 230–241 (2016)
10. Zhang, F, Ju, P, Pan, M, Zhang, D, Huang, Y, Li, G, Li, X, ''Self-healing Mechanisms in Smart Protective Coatings: A Review.'' *Corros. Sci.*, **144** 74–88 (2018)
11. Zhang, D, Ronson, TK, Nitschke, JR, ''Functional Capsules via Subcomponent Selfassembly.'' *Acc. Chem. Res.*, **51** 2423–2436 (2018)
12. Javidparvar, AA, Ramezanzadeh, B, Ghasemi, E, ''Effect of Various Spinel Ferrite Nanopigments Modified by Amino Propyl Trimethoxy Silane on the Corrosion Inhibition Properties of the Epoxy Nanocomposites.'' *Corrosion*, **72** (6) 761–774 (2016)
13. Chaudhry, AU, Mittal, V, Mishra, B, ''Nano Nickel Ferrite ($NiFe_2O_4$) as Anticorrosion Pigment for API 5L X-80 Steel: An Electrochemical Study in Acidic and Saline Media.'' *Dyes Pigm.*, **118** 18–26 (2015)
14. Ghaffari, MS, Naderi, R, Sayehbani, M, ''The Effect of Mixture of Mercaptobenzimidazole and Zinc Phosphate on the Corrosion Protection of Epoxy/Polyamide Coating.'' *Prog. Org. Coat.*, **86** 117–124 (2015)
15. Ramezanzadeh, B, Akbarian, M, Ramezanzadeh, M, Mahdavian, M, Alibakhshi, E, Kardar, P, ''Corrosion Protection of Steel with Zinc Phosphate Conversion Coating and Post-

treatment by Hybrid Organic-Inorganic Sol-Gel Based Silane Film.'' *J. Electrochem. Soc.*, **164** (6) C224 (2017)
16. Zheludkevich, ML, Tedim, J, Ferreira, MGS, '''Smart' Coatings for Active Corrosion Protection Based on Multi-functional Micro and Nanocontainers.'' *Electrochim. Acta*, **82** 314–323 (2012)
17. Behzadnasab, M, Mirabedini, SM, Kabiri, K, Jamali, S, ''Corrosion Performance of Epoxy Coatings Containing Silane Treated ZrO_2 Nanoparticles on Mild Steel in 3.5% NaCl Solution.'' *Corros. Sci.*, **53** (1) 89–98 (2011)
18. Chen, T, Chen, R, Jin, Z, Liu, J, ''Engineering Hollow Mesoporous Silica Nanocontainers with Molecular Switches for Continuous Self-healing Anticorrosion Coating.'' *J. Mater. Chem. A*, **3** (18) 9510–9516 (2015)
19. Shchukina, E, Shchukin, D, Grigoriev, D, ''Effect of Inhibitor-Loaded Halloysites and Mesoporous Silica Nanocontainers on Corrosion Protection of Powder Coatings.'' *Prog. Org. Coat.*, **102** 60–65 (2017)
20. Zahidah, KA, Kakooei, S, Ismail, MC, Bothi Raja, P, ''Halloysite Nanotubes as Nanocontainer for Smart Coating Application: A Review.'' *Prog. Org. Coat.*, **111** 175–185 (2017)
21. Haddadi, SA, Mahdavian, M, Karimi, E, ''Evaluation of the Corrosion Protection Properties of an Epoxy Coating Containing Sol–Gel Surface Modified Nano-Zirconia on Mild Steel.'' *RSC Adv.*, **5** (36) 28769–28777 (2015)
22. Tedim, J, Zheludkevich, ML, Bastos, AC, Salak, AN, Lisenkov, AD, Ferreira, MGS, ''Influence of Preparation Conditions of Layered Double Hydroxide Conversion Films on Corrosion Protection.'' *Electrochim. Acta*, **117** 164–171 (2014)
23. Hayatdavoudi, H, Rahsepar, M, ''Smart Inhibition Action of Layered Double Hydroxide Nanocontainers in Zinc-Rich Epoxy Coating for Active Corrosion Protection of Carbon Steel Substrate.'' *J. Alloys Compd.*, **711** 560–567 (2017)
24. Alibakhshi, E, Ghasemi, E, Mahdavian, M, Ramezanzadeh, B, Farashi, S, ''Active Corrosion Protection of Mg-Al-PO_4^{3-} LDH Nanoparticle in Silane Primer Coated with Epoxy on Mild Steel.'' *J. Taiwan Inst. Chem. Eng.*, **75** 248–262 (2017)
25. Iqbal, MA, Sun, L, Barrett, AT, Fedel, M, ''Layered Double Hydroxide Protective Films Developed on Aluminum and Aluminum Alloys: Synthetic Methods and Anticorrosion Mechanisms.'' *Coatings*, **10** (4) 428 (2020)
26. Iqbal, MA, Secchi, M, Iqbal, MA, Montagna, M, Zanella, C, Fedel, M, ''MgAl-LDH/Graphene Protective Film: Insight into LDH-Graphene Interaction.'' *Surf. Coat. Technol.*, **401** 126253 (2020)
27. Liu, XW, Xiong, JP, Lv, YW, Zuo, Y, ''Study on Corrosion Electrochemical Behavior of Several Different coating Systems by EIS.'' *Prog. Org. Coat.*, **64** (4) 497–503 (2009)
28. Hou, J, Zhu, G, Xu, JK, Liu, HJ, ''Anticorrosion Performance of Epoxy Coatings Containing Small Amount of Inherently Conducting PEDOT/PSS on Hull Steel in Seawater.'' *J. Mater. Sci. Technol.*, **29** (7) 678–684 (2013)
29. Zhang, F, Sun, M, Sailong, X, Zhao, L, Zhang, B, ''Fabrication of Oriented Layered Double Hydroxide Films by Spin Coating and Their Use in Corrosion Protection.'' *Chem. Eng. J.*, **141** (1–3) 362–367 (2008)
30. Tabish, M, Zhao, J, Wang, J, Anjum, MJ, Qiang, Y, Yang, Q, Mushtaq, MA, Yasin, G, ''Improving the Corrosion Protection Ability of Epoxy Coating Using CaAl LDH Intercalated with 2-Mercaptobenzothiazole as a Pigment on Steel Substrate.'' *Prog. Org. Coat.*, **165** 106765 (2022)
31. Holzner, T, Luckeneder, G, Strauß, B, Valtiner, M, ''Environmentally Friendly Layered Double Hydroxide Conversion Layers: Formation Kinetics on Zn–Al–Mg-Coated Steel.'' *ACS Appl. Mater. Interfaces*, **14** (4) 6109–6119 (2022)
32. Dong, B, Chen, P, Xiao, B, Zeng, L, Zhao, M, Hong, S, ''Growth Mechanism and Corrosion Resistance of a Co-Al Layered Double Hydroxide Film Grown In Situ on a Steel Substrate.'' *J. Mater. Civ. Eng.*, **35** (4) 04023031 (2023)
33. Idouhli, R, Abouelfida, A, Benyaich, A, Aityoub, A, ''*Cuminum cyminum* Extract: A Green Corrosion Inhibitor of S300 Steel in 1 M HCl.'' *Chem. Process Eng. Res.*, **44** 16–25 (2016)
34. Znini, M, Majidi, L, Bouyanzer, A, et al. ''Essential Oil of *Salvia aucheri mesatlantica* as a Green Inhibitor for the Corrosion of Steel in 0.5 M H_2SO_4.'' *Arab. J. Chem.*, **5** 467–474 (2012)
35. Idouhli, R, Oukhrib, A, Koumya, Y, et al. ''Inhibitory Effect of Atlas Cedar Essential Oil on the Corrosion of Steel in 1 M HCl.'' *Corros. Rev.*, **36** 373–384 (2018)
36. Vermaa, CB, Quraishia, MA, Singh, A, ''2-Aminobenzene-1,3-Dicarbonitriles as Green Corrosion Inhibitor for Mild Steel in 1 M HCl: Electrochemical, Thermodynamic, Surface and Quantum Chemical Investigation.'' *J. Taiwan Inst. Chem. Eng.*, **49** 229–239 (2015)
37. Leal, DA, Sousa, I, Bastos, AC, Tedim, J, Wypych, F, Marino, CEB, ''Combination of Layered-Based Materials as an Innovative Strategy for Improving Active Corrosion Protection of Carbon Steel.'' *Surf. Coat. Technol.*, **473** 129972 (2023)
38. Touir, R, Cenoui, M, El Bakri, M, Ebn Touhami, M, ''Sodium Gluconate as Corrosion and Scale Inhibitor of Ordinary Steel in Simulated Cooling Water.'' *Corros. Sci.*, **50** (6) 1530–1537 (2008)
39. Powell, SM, McMurray, H, Worsley, D, ''Use of the Scanning Reference Electrode Technique for the Evaluation of Environmentally Friendly, Nonchromate Corrosion Inhibitors.'' *Corrosion*, **55** 1040–1051 (1999)
40. Wang, H, Zheng, J, ''Progress of Research on Environmental-Friendly Corrosion Inhibitors.'' *Corros. Sci. Prot. Technol.*, **14** 275–279 (2002)
41. Renaudin, G, Francois, M, Evrard, O, ''Order and Disorder in the Lamellar Hydrated Tetracalcium Monocarboaluminate Compound.'' *Cem. Concrete Res.*, **29** (1) 63–69 (1999)
42. Szabados, M, Mészáros, R, Erdei, S, Kónya, Z, Kukovecz, Á, Sipos, P, Pálinkó, I, ''Ultrasonically-Enhanced Mechanochemical Synthesis of CaAl-Layered Double Hydroxides Intercalated by a Variety of Inorganic Anions.'' *Ultrason. Sonochem.*, **31** 409–416 (2016)
43. Serdechnova, M, Salak, AN, Barbosa, FS, Vieira, DEL, Tedim, J, Zheludkevich, ML, Ferreira, MGS, ''Interlayer Intercalation and Arrangement of 2-Mercaptobenzothiazolate and 1, 2, 3-Benzotriazolate Anions in Layered Double Hydroxides: In Situ X-ray Diffraction Study.'' *J. Solid State Chem.*, **233** 158–165 (2016)
44. Wu, CH, Chang, YP, Chen, SY, Liu, DM, Yu, CT, Pen, BL, ''Characterization and Structure Evolution of Ca–Al–CO_3 Hydrotalcite Film for High Temperature CO_2 Adsorption.'' *J. Nanosci. Nanotechnol.*, **10** (7) 4716–4720 (2010)
45. Zhang, Y, Li, L, Shi, D, Song, F, ''Synthesis and Application of Low-Cost Layered Double Hydroxides Intercalated by Gluconic Acid anion for Flame Retardancy and Tensile Strength Conservation of High Filling Epoxy Resin.'' *J. Colloid Interface Sci.*, **594** 791–801 (2021)
46. Saiah, FB, Djellal, B-LS, Bettahar, N, ''Nickel–Iron Layered Double Hydroxide (LDH): Textural Properties Upon Hydrothermal Treatments and Application on Dye Sorption.'' *J. Hazard. Mater.*, **165** (1–3) 206–217 (2009)
47. Benício, LP, Figueredo, DE, de Moura, L, Guimarães, FG, Pinto, LM, da Costa, J, Tronto, ''Layered Double Hydrox-

ides as Hosting Matrices for Storage and Slow Release of Phosphate Analyzed by Stirred-Flow Method.'' *Mater. Res.*, **21** 20171004 (2018)
48. Stuart, BH, *Infrared Spectroscopy: Fundamentals and Applications*. John Wiley & Sons (2004)
49. Wang, D-Y, Costa, FR, Vyalikh, A, Leuteritz, A, Scheler, U, Jehnichen, D, Wagenknecht, U, Häussler, L, Heinrich, G, ''One-Step Synthesis of Organic LDH and its Comparison with Regeneration and Anion Exchange Method.'' *Chem. Mater.*, **21** (19) 4490–4497 (2009)
50. Galvão, TLP, Neves, CS, Zheludkevich, ML, Gomes, JRB, Tedim, J, Ferreira, MGS, ''How Density Functional Theory Surface Energies May Explain the Morphology of Particles, Nanosheets, and Conversion Films Based on Layered Double Hydroxides.'' *J. Phys. Chem. C*, **121** (4) 2211–2220 (2017)
51. Huet, F, ''Electrochemical Noise Technique.'' *Corros. Technol. New York Basel*, **22** 507 (2006)
52. Sushkova, A, Montes, R, Paulino, T, Sousa, I, Neves, C, Ferreira, MG, Tedim, J, ''A Novel Smart Coating with Hexacyanoferrate Intercalated Layered Double Hydroxides Nanoadditive for Early Detection of Carbon Steel Corrosion.'' *Front. Chem. Eng.*, **5** 1145049 (2023)
53. Hsu, CH, Mansfeld, F, ''Concerning the Conversion of the Constant Phase Element Parameter Y0 into a Capacitance.'' *Corrosion*, **57** (9) 747 (2001)